GEOPHYSICAL RESEARCH LETTERS, VOL. 27, NO. 24, PAGES 4013-4016, DECEMBER 15, 2000

Hemispheric asymmetries in ionospheric electrodynamics during the solar wind void of 11 May 1999

D. J. Knipp,[1] C.-H. Lin,[2] B. A. Emery,[3] J. M. Ruohoniemi,[4] F. J. Rich,[5] and D. S. Evans[6]

Abstract. We use the Assimilative Mapping of Ionospheric Electrodynamics (AMIE) procedure to produce composite maps of high-latitude ionospheric parameters for 11 May 1999. On that day there was a near void in the solar wind momentum flux. Yet, focused high-latitude interactions occurred at Earth. Our maps of convection, Joule heating, particle precipitating power and field-aligned current show a striking asymmetry between hemispheres. In the latter three parameters there is at least a five-fold difference in values between the hemispheres. The northern hemisphere polar cap particle precipitation is the strongest we have ever mapped. Strong electrodynamic interactions were focused above 70° north magnetic latitude. In the southern hemisphere only weak, irregular patterns are mapped. We attribute these differences to the strong interplanetary magnetic field spiral configuration, the sunward tilt of the northern hemisphere and the direct beam or "strahl" of solar electrons impinging on the northern polar cap during the momentum void.

1. Background

On 11 May 1999 both ACE and WIND satellites observed the solar wind density and velocity to be unusually low with an average number density less than 1/cm^{-3} and an average speed of ~ 350 km/s. As shown in Figure 1, this void was accompanied by a spiral or 'away' orientation of the IMF (B_x -, B_y +, B_z ~0). According to anti-parallel merging theory [*Crooker,* 1988], merging between the interplanetary magnetic field (IMF) and the magnetosphere lobe field lines during intervals of strong spiral IMF orientation can contribute to imbalances in what is normally nearly-symmetric two-cell convection in the ionosphere and magnetosphere. The theory also implies that significant interhemispheric differences can develop as the result of dipole tilting. During extreme situations, such as the one we discuss here, the convection may develop into a round/crescent structuring or collapse to a single-cell in one hemisphere and a weak irregular convection system in the other hemisphere, especially if large conductivity asymmetries are present [*Knipp et al.,* 1993]. *Fairfield and Scudder* [1985] report another possible asymmetry associated with the 'away' oriented IMF: fluxes of solar electrons aligned with the IMF should have preferential access to the northern polar cap. Dipole tilting can further enhance this effect, as well. The events of 11 May 1999 allow a view of how unusual solar wind, merging, and particle precipitation phenomena can combine to produce extreme responses in the ionosphere and extraordinary interhemispheric differences.

The Assimilative Mapping of Ionospheric Electrodynamics (AMIE) procedure is a constrained, weighted, least-squares fit of ionospheric electrodynamic parameters to a variety of ground- and space-based data [*Richmond and Kamide,* 1988]. Typically the procedure is run with 5 to 30 min time resolution producing snapshots of ionospheric convection, currents and conductance to study high-latitude disturbances in the geo-space environment. Here, instead of snapshots, we produce 'composite' views of the electrodynamic system by assimilating data over an 11-hr interval centered on 1430 UT.

We have investigated the validity of such a long-interval mapping. The IMF components were relatively steady during the 11-hr period (Fig 1). AMIE maps from individual 30-min intervals (not shown) suggest minimal large-scale ionospheric variations and confirm the presence of the large-scale features we illustrate in this study. However, higher resolution maps, which will be discussed in a future paper, show some of the small-scale variations reported by *Papitashvili et al.* [2000].

2. Data

The multi-hour window allows us to accumulate data from several hundred points along polar orbiting satellite tracks and from thousands of radar observations. We also incorporate data from sensors on the polar orbiting Defense Meteorological Satellite Program (DMSP) and NOAA satellites that measure downward flux and mean energy of precipitating electrons in the range of 30 eV to 300 keV. DMSP ion drifts

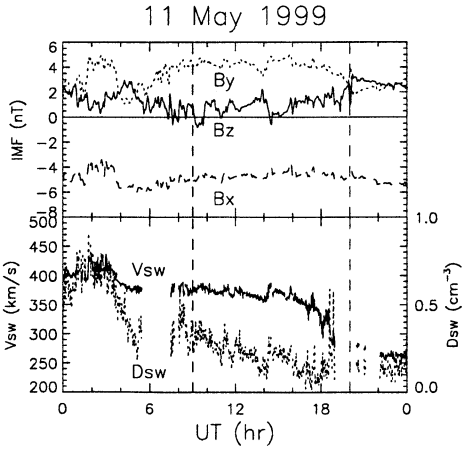

Figure 1. ACE solar wind observations in GSM coordinates for May 11 1999 at 224R_E. B_y (…), B_z (—), B_x (---), velocity (dark), density (light). The density scale is on the right.

[1]Department of Physics US Air Force Academy, Colorado, USA
[2]National Central University, Chung-Li, Taiwan
[3]High Altitude Observatory, NCAR, Boulder, Colorado, USA
[4]The Johns Hopkins University, Applied Physics Laboratory, Laurel, Maryland, USA
[5]Space Vehicles Directorate, Hanscom AFB, Massachusetts, USA
[6]Space Environment Center, Boulder Colorado, USA

Paper number 2000GL003801.
0094-8276/00/1999GL003801$05.00

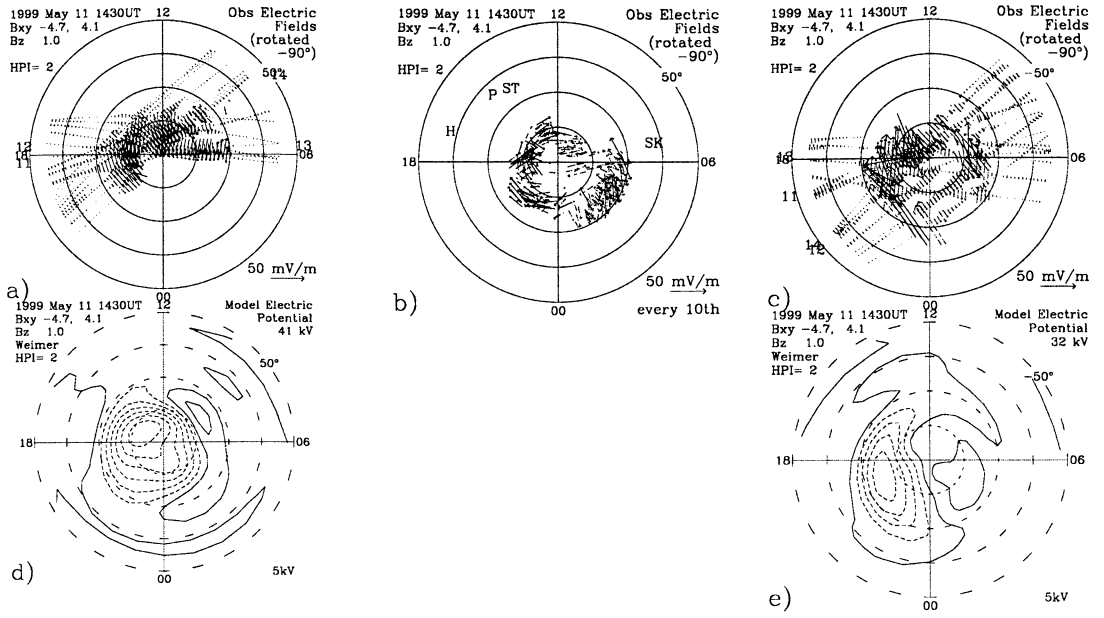

Figure 2. Data input for 11 May 1999. a) Ion drifts from northern hemisphere DMSP satellites. The vector in the lower left of the observation plots represents electric field strength of 50 mV/m. b) Plasma drifts observed by five SuperDARN radars. Locations for Kapuskasing, and Saskatoon, Canada, Stokkseyri, and Pykkvibær, Iceland, and Hankasalmi, Finland are shown for the end of the mapping interval. For clarity only every tenth line-of-site observation is displayed. c) Ion drifts observed by DMSP satellites in the southern hemisphere. The Weimer statistical pattern used as *a priori* information for the d) Northern and e) Southern hemisphere. Contour intervals are 5 kV.

(Figs. 2a and 2c) are mapped along geomagnetic field lines, scaled to a reference altitude of 110 km and converted to electric fields. Similarly the drift of decameter scale ionospheric irregularities measured by five northern hemisphere Super Dual Auroral Radar Network (SuperDARN) radars (Fig. 2b) are also converted to electric field observations for assimilation. We have assimilated all direct electric field observations currently available. Although fewer data are available in the southern hemisphere, we believe the breadth of coverage there is sufficient for this study. In regions of poor data coverage the mapped patterns are influenced by the *a priori* statistical patterns of *Weimer* [1996].

Figures 2d and 2e show the northern and southern hemisphere statistical electric potential patterns for the average IMF and dipole tilt values associated with this 11-hr interval. With B_z and B_y both positive, but $|B_y| > |B_z|$, the northern sunward-titled hemisphere shows a two-cell configuration for the electric potential pattern with most of the potential in the negative dusk cell. The southern anti-sunward-tilted hemisphere presents a weaker convection system with a more crescent-shaped, but still dominant dusk cell. The dominance of the dusk cell under IMF B_y positive conditions is a feature of all IMF-based statistical models.

3. Results and Discussion

An initial objective of this study was to simply determine what ionospheric behavior, if any, takes place under conditions of minimal solar wind. Many interesting features arose. Figure 3 shows the northern and southern electrodynamic maps in the left and right columns, respectively, for the interval surrounding 1430 UT. Figures 3a and 3b show the electric potential (or plasma convection) patterns. Despite the similar cross polar voltage values in the two hemispheres (35 kV for the north and 33 kV for the south) there is a fundamental difference in the configurations. The northern pattern is a tight, single vortex with a center above 80° magnetic latitude (MLAT). In the southern hemisphere the electric field is generally weaker and maps to a more latitudinally-extended pattern. The field-aligned currents show even larger interhemispheric differences. In the north (Fig. 3c) there are sheet-like current structures with unusually intense currents in the center of the polar cap. In the south only weak filamentary structures appear (Fig. 3d). (Note that it is necessary to have different current contour levels for the two hemispheres because of the weak currents in the south). There is a factor-of-seven difference in the magnitude of the integrated downward (and upward) field-aligned currents in the two hemispheres. A large interhemispheric difference also exists in the integrated Joule heating (Figs. 3e and 3f). In the north the Joule heating is focused above 80° and is roughly ten times larger than that in the south. Finally, the comparison for particle energy flux (Figs. 3g and 3h) reveals a northern polar cap filled with electron precipitation but a southern polar cap devoid of such. Only weak auroral zone precipitation is present in the south. Energy flux into the northern hemisphere is a factor-of-five greater than that in the southern hemisphere. The total energy dissipation rate in the northern hemisphere (Joule heating plus particle heating) was ~60 GW compared to ~8 GW in the southern hemisphere.

Are these multi-hour composite patterns realistic? If so, what are the primary influences that produce such asymmetrical patterns? The answer to the first question is yes. Composite ground magnetometer data, used alone as an independ-

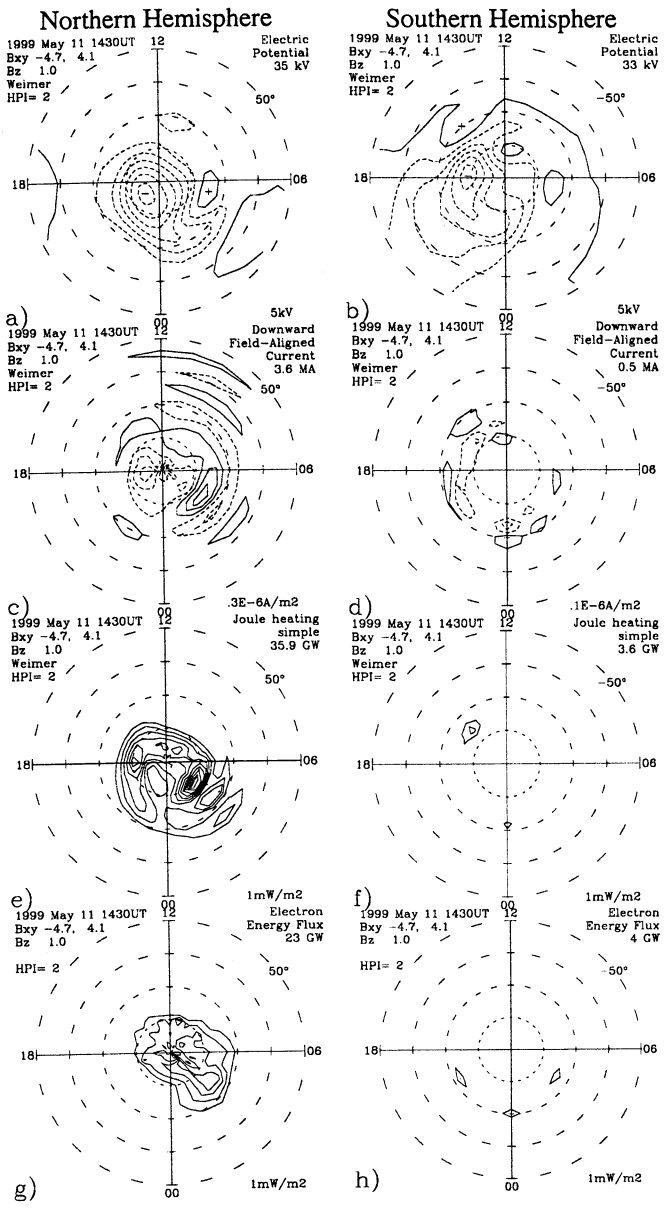

Figure 3. Mapped patterns for 11 May 1999. The maps are centered on 1430 UT but represent the interval from 0900-2000 UT. All northern hemisphere plots look down on the north pole. All southern hemisphere plots look through the earth and view the south from inside the earth. The outer ring corresponds to +/-50° MLAT. Hemispherically integrated values are shown in the upper right corners of the field-aligned current, Joule heating and particle energy flux plots. a) Northern and b) Southern hemisphere fitted electric potential pattern with the cross polar voltage given in the upper right corner. The contour interval is 5kV. c) Northern and d) Southern hemisphere fitted field-aligned current. Solid (dashed) lines indicate downward (upward) field-aligned currents. The contour interval is 0.3 $\mu A/m^2$ for the north and 0.1 $\mu A/m^2$ for the south. The globally integrated downward field-aligned current is 3.5 Mega-Amperes (MA) for the north and 0.6 MA for the south. e) Northern and f) Southern hemisphere Joule heating distribution. The contour interval is $1 mW/m^2$. g) Northern and f) Southern hemisphere particle energy flux. The contour interval is 1 mW/m^2.

ent assimilation, give a similar, albeit weaker, configuration for the northern convection pattern. Data from the ØRSTED satellite [Papitashvili et al., this issue] and from the IRIDIUM satellite constellation [B. Anderson, private communication] confirm, for both hemispheres, the field-aligned current configurations we show here. There are no direct measures of Joule heating, but a recent statistical analysis [Chun et al., work in progress] shows that Joule heating can be confined to very high-latitudes during summer events when strong electric fields dominate due to lobe merging. Our northern particle precipitation pattern is consistent with the strahl of electrons that produce the intense polar rain observed by the DMSP, NOAA and POLAR satellites. The absence of strong particle precipitation in the southern hemisphere is also consistent with satellite observations. However, optical data from McMurdo, Antarctica indicate weakly varying auroral emissions in the southern hemisphere [*Weatherwax et al.*, 2000]. Thus, the southern hemisphere was not fully quiet.

The pattern for the northern particle precipitation is unlike any we previously have mapped in intensity, localization and duration. Generally the mapped particle energy flux patterns conform to the shape of the auroral oval. The difference for this event appears to be associated with the reported beam of direct solar coronal electrons impinging on the near earth environment [P. Anderson, private communication]. Electron precipitation data incorporated into our maps are from lower energies than those discussed by Anderson et al., but the timing and location of the particle deposition suggest that lower energy electrons were part of the strahl reported from instruments on the POLAR satellite. The effect of the electron beam is: 1) to generate the obvious interhemispheric difference in particle precipitation, 2) to increase conductance (not shown) above the background solar ionization component, thus, increasing Joule heating energy dissipation and 3) to contribute to the intense upward field-aligned current in the northern polar cap [*Papitashvili et al.*, 2000].

What of the asymmetries? We might expect imbalances in the convection patterns based on the IMF orientation and season based on anti-parallel merging theory and as shown in Figures 2e and 2d. The IMF and dipole configurations were favorable for merging on the north dusk lobe of the magnetosphere. The north field-aligned current pattern (Fig. 2d) is consistent with the statistical result presented by *Friis Chrsitensen et al.*, [1985] for 'away' sector IMF orientation. Thus, the IMF and dipole orientations could account for part of the unusual northern hemisphere patterns. But, as a matter of completeness we cannot rule out the documented expansion of the magnetosphere as a contributor to the unusual electrodynamic state on this date. A significant inflation of the magnetosphere during the momentum void could have presented the opportunity for abnormal merging configurations. A broader, more integrated ionosphere-magnetosphere study is required to assess the impact of the magnetospheric inflation.

The southern hemisphere appears to be less controlled by the spiral IMF orientation and uninfluenced by the strahl event. The convection pattern is broader than in the north. Some of the broadening may be due to more variable geomagnetic activity in the southern hemisphere which could lead to pattern 'smearing' in the composite maps. There are fewer data for the southern hemisphere maps so the Weimer *a priori* pattern of the electric potential may have a larger influence there. The strong electric field in the post-noon region is due to fitting to ion drifts that varied significantly between

satellite passes. Both temporal and spatial variability are contributing to enhanced field strength in that region. We also know from previous work [*Knipp et al.,* 1993] that electric fields in the dark wintertime hemisphere are less organized than those in the sunlit hemisphere, thus making large-scale mapping somewhat less reliable. There are conductivity influences present in all of patterns. The southern hemisphere field-aligned current strength is less than 20% of that in the north, consistent with the contrast in conductivity. The absence of solar and strahl-induced conductance and the weaker auroral conductance are mostly responsible for the reduced Joule heating in the southern hemisphere.

4. Conclusions

Conditions in the interplanetary medium were sufficiently stable to allow a composite mapping of ionospheric electrodynamics in an 11-hour interval surrounding 1430 UT on 11 May 1999 using the AMIE procedure. During the momentum flux void significant electrodynamic interactions took place between the interplanetary medium and the Earth. Data assimilation over the interval reveals that significant asymmetries existed in the high-latitude ionosphere. Within the northern hemisphere the patterns show electrodynamic interactions focused on the polar cap and extending to roughly 70 MLAT. A single convection cell dominates in the northern hemisphere. In the southern hemisphere the convection is broader and generally more diffuse. While the cross-polar voltages are similar between the hemispheres (35 kV in the north and 33 kV in the south), there is at least a five-fold difference in the interhemispheric strengths of field-aligned currents, Joule heating and particle precipitation power. The spiral IMF orientation, the sunward tilt of the northern hemisphere, and the strahl of coronal electrons likely played a role in the enhancement of these quantities in the northern hemisphere. By the same token the absence of these factors for the southern hemisphere produced a quieter ionospheric state.

Acknowledgments. D. Knipp and B. Emery were funded by NSF grant ATM 9613829. D. Knipp was also funded by NASA Award W-17384. The operation of the SuperDARN radars in the northern hemisphere is supported by the national funding agencies of the U.S., Canada, the U.K. and France. D. Weimer provided statistical patterns for the mapping. ACE Level 2 Solar Wind data were provided by the ACE Science Center at Cal Tech. We acknowledge useful discussions with M. G. McHarg and A. D. Richmond.

References

Crooker, N. U. Mapping the merging potential from the magnetosphere to the ionosphere through the dayside cusp, *J. Geophys. Res., 93*, 7338, 1988.

Friis Christensen, E., Y. Kamide, A. D. Richmond and S. Matsushita, Interplanetary magnetic field control of high-latitude electric fields and currents determined from Greenland magnetometer data, *J. Geophys Res., 90*, 1325, 1985.

Fairfield, D. H. and J. D. Scudder, Polar Rain: Solar coronal electrons in the earth's magnetosphere, *J. Geophys. Res., 90,* 4055, 1985.

Knipp, D. J. et al., Ionospheric response to slow, strong variations during northward interplanetary magnetic field: A case study for 14 January 1988, *J. Geophys. Res., 98*, 19273, 1993.

Papitashvili, et al., Geomagnetic disturbances at high-latitudes during very low solar wind density event, this issue.

Richmond, A. D., and Y. Kamide, Mapping Ionospheric electrodynamic features of the high-latitude ionosphere from localized observations: Technique. *J. Geophys. Res., 93*, 5741, 1988.

Weatherwax, A., et al., The distention of the magnetosphere on May 11 1999: High latitude Antarctic observations and comparisons with low latitude magnetic and geopotential data, this issue.

Weimer, D. R., A flexible, IMF dependent model of high-latitude electric potentials having "space weather" applications, *Geophys. Res. Lett, 23*, 2549, 1996.

D. J. Knipp, Department of Physics, US Air Force Academy, Colorado, USA, 80840. (e-mail: delores.knipp@usafa.af.mil).

C.-H. Lin, National Central University, Chung-Li, Taiwan. (e-mail: chlin@sedc.ss.ncu.edu.tw).

B. A. Emery, High Altitude Observatory, NCAR, Boulder, Colorado, USA, 80301 (e-mail: emery@ucar.edu).

J. M. Ruohoniemi, The Johns Hopkins University, Applied Physics Laboratory, Laurel, Maryland, USA, 20723. (e-mail: Mike.Ruohoniemi@jhuapl.edu).

F. J. Rich, AFRL/VSBP, Hanscom Air Force Base, Massachusetts, USA 01731. (e-mail:frederick.rich@hanscom.af.mil)

D. S. Evans, Space Environment Center, Boulder, Colorado, USA, 80303. (e-mail: devans@sec.noaa.gov).

(Received April 15, 2000; revised June 5, 2000;
accepted June 9, 2000.)